Photoelectron spectra of conducting polymers–molecularly doped polyacetylenes

H. R. Thomas, W. R. Salaneck, C. B. Duke
Xerox Webster Research Center, Xerox Square, W-114, Rochester, New York, 14644, USA

and E. W. Plummer*, A. J. Heeger* and A. G. MacDiarmid†
Laboratory for Research on the Structure of Matter‡, University of Pennsylvania, Philadelphia, Pennsylvania 19104, USA
(Received 29 April 1980)

Polyacetylene, $(CH)_x$, is one of the simplest of the conjugated organic polymers and is, therefore, of fundamental importance in the theoretical and spectroscopic studies of unsaturated polymer systems. The electrons from the unsaturated pi system are delocalized along the polymer chain. If all of the C–C bond lengths were equal, these pi electrons would be expected to exhibit metallic behaviour. Due to the effects of bond alternation and Coulomb correlations, however, an energy gap occurs in the electronic excitation spectrum leading to semiconducting behaviour. Recent studies have demonstrated that doping of the $(CH)_x$ with a variety of doners and acceptors gives *n*- and *p*-type semiconductors. When the dopant concentration reaches a few mol percent, the doped $(CH)_x$ films undergo a semiconductor-to-metal transition.

Following a brief indication of current research on the polyacetylenes, in this paper we present photoemission spectra and X-ray-induced Auger electron spectra for pure polyacetylene, as well as for AsF_5 and iodine doped polyacetylene. In the case of AsF_5 doping, at concentrations near that leading to the maximum electrical conductivity (~11% AsF_5), the As:F ratio is 1:5 and the arsenic–fluoride moieties are localized near the surface of the polyacetylene fibrils. The C_{1s} core-level spectra indicate a charge transfer of one electron per AsF_5 molecule. The u.p.s. spectra, the X-ray induced Auger spectra and CNDO calculations suggest, however, that the AsF_5 moieties are not simple AsF_5^- radical anions. In the case of iodine doped $(CH)_x$, the dopant concentration is more nearly uniform and I_5^- appears to be the relevant anion species. The inhomogeneity of the doped samples constitutes the greatest barrier to a quantitative interpretation of the photoemission spectra using simple theoretical models.

INTRODUCTION

It has been shown that upon exposure to electronegative molecular dopants, the electrical conductivity of free standing films of polyacetylene[1-3], which we refer to as $(CH)_x$, increases by almost twelve orders of magnitude[4-8]. A prerequisite to the understanding of the conductivity mechanism(s) is the delineation of the role of the dopants in highly conducting $(CH)_x$. Although the high conductivity results from charge transfer between the dopant and the $(CH)_x$, the detailed nature of this charge transfer is not clear. In traditional one-electron models the acceptor (donor) captures (gives up) an electron from the valence band (to the conduction band) and the resulting charged species traps the hole left behind (the donated electron). As the doping increases, these trapped holes (electrons) become more numerous until eventually they screen the charged acceptors' (donors') coulomb attraction sufficiently effectively that a semiconductor-to-metal transition occurs. Alternatively, if the $(CH)_x$ macromolecules exhibit a collective ground state, known as a charge–density–wave state, then doping can induce charged domain walls, called solitons, instead of electrons or holes[9,10]. If such is the case, then the physical mechanism of the charge transfer in $(CH)_x$ differs considerably from that in conventional network semiconducters like silicon. The nature of the dopant-host interaction and the semiconductor-to-metal transition in $(CH)_x$ could be qualitatively different from that known in other systems, although a truly convincing demonstration of the validity of this hypothesis has not yet been given. An extensive review of the various types of models and the experimental evidence for the validity of each has been given by Duke[11].

We have approached this problem by examining the electronic structure of molecularly doped $(CH)_x$ via the use of photoelectron and Auger electron spectroscopy. In this paper, we report the ultraviolet and X-ray photoelectron spectra (u.p.s. and X.p.s., respectively) of AsF_5 and Iodine doped $(CH)_x$. In particular, we have studied the electronic structure of pure, AsF_5 and iodine doped polycrystalline polyacetylene, i.e. $[CH(AsF_5)_y]_x$ for $y=0.11$, and $(CHI_y)_x$ for $y=0$, 0.05, 0.12, 0.24 and 0.28. Insight into the significance of the energies and intensities of structure in the u.p.s. and X.p.s. spectra of the doped polymer films is gained via comparison of these data with corresponding spectra of gaseous and condensed films of AsF_3 and AsF_5 molecules, of crushed powder samples of

* Department of Physics
† Department of Chemistry
‡ Work at the University of Pennsylvania was supported by the NSF Materials Research Laboratory under grant DMR-76-80994

0032-3861/80/111238-09$02.00

the $Na^+AsF_6^-$ salt, and of gaseous and condensed molecular solid phases of I_2, as well as with model CNDO molecular orbital calculations.

Our results are presented in two sections. In the first, for the AsF_5 molecular dopant the core-level and valence-level spectra for $[CH(AsF_5)_{0.11}]_x$ are presented and interpreted with the use of data from AsF_3, AsF_5 and $Na^+AsF_6^-$. The value $y=0.11$ (i.e., 11%) corresponds to the doping level at which the electrical conductivity has reached a maximum. Secondly, for the iodine doped $(CH)_x$ the trends in the data were independent of initial iodine concentration. Therefore only the 0.05 and 0.28 data are presented. An understanding of the significance of the features of the photoelectron spectra is gained through a comparison with the corresponding spectra of gaseous and the condensed molecular soled phases of I_2, as well as with the spectra for AsF_5-doped $(CH)_x$.

EXPERIMENTAL

The fibrous $(CH)_x$ films used in this work were prepared by the polymerization of acetylene over a Ziegler–Natta catalyst, the procedure for which is described elsewhere[1-3]. The typical fibril diameter was nominally 200 Å, as determined by electron microscopy. Because of the thermal history of our films, all samples studied were of the *trans* stereo isomer. Doping was accomplished by exposing $(CH)_x$ freestanding films to a vapour of AsF_5 or I_2 as reported elsewhere[4,5]. The doping level (y-value) was determined by bulk chemical analysis, by weight increase, or by electrical conductivity curves generated previously on samples for which a bulk chemical analysis had been performed. The photoelectron spectra were recorded between -100°C and room temperature in an AEI ES 200B photoelectron spectrometer, employing an AEI monochromatized AL $K\alpha_{1,2}$ X-ray source (1486.7 eV photons), an unfiltered $MgK\alpha_{1,2}$ source (1253.7 eV photons), and a Vacuum Generators (V.G) windowless ultraviolet source (21.2 eV photons and 40.8 eV photons) coupled to a V.G. grazing incidence u.v. monochromator. The electrons were collected at near-normal exit from the sample. Our results are independent of take-off angle of the electrons, because of the fibril nature of the samples[1,2].

The AEI instrument is fitted with insertion locks, which allow samples to go from atmospheric pressure to 10^{-6} Torr in about one minute, and ultimately to lower 10^{-8} Torr without bakeout. Samples were mounted on the sample probe in a dry N_2 atmosphere in a glove box prior to insertion into the spectrometer. The O_2 content of the N_2 atmosphere was <8 ppm, and the H_2O content was reduced to below detectable limits by passing the N_2 gas over a copper coil whose surface was cooled by flowing liquid nitrogen within the coil. Gas phase X.p.s. studies were accomplished using the standard AEI gas cell.

A few interesting experimental sample handling observations include the following[1,2]:

(1) When exposed to air, undoped $(CH)_x$ picks up oxygen contamination. Samples can be washed in chloroform to remove the surface contamination. Clean surfaces are reproduced when the wet samples are inserted very quickly into a high vacuum environment.

(2) The AsF_5 does not pump off in the vacuum system (the carbon: arsenic: fluorine ratios remain essentially constant at room temperature over a period of several days at pressures down to below 10^{-8} Torr).

(3) The spectra do not change with time in the spectrometer, in contrast to the case of AsF_5-intercalated graphite, where the As and F signals initially decrease with time at room temperature.

(4) Exposure of the AsF_5-doped samples to air for up to 5 min does not lead to any significant increase in the surface oxygen content, whereas pure AsF_5 reacts instantly with water vapour when exposed to laboratory air.

In the case of the iodine-doped polymers, samples were run first at low temperatures, then allowed to stand at room temperature in the spectrometer vacuum environment overnight at least, then rerun. Relative to the C(1s) signal, the iodine signal always decreased after the room temperature pumping. Details are found in the section on the iodine doped $(CH)_x$.

RESULTS

$[CH(AsF_5)_y]_x$ *for* y = 0.11

(1) Core level spectra: X.p.s. core-level spectra are used to establish the atomic composition near the surface, the depth distribution from the surface of adsorbed species resulting from the exposure of $(CH)_x$ films to AsF_5 molecular vapour, and the charge transfer between the $(CH)_x$ macromolecules and the molecular dopant. Instrument sensitivity to the various arsenic and fluorine core-levels was determined through the AsF_3 and AsF_5 gas and condensed phase X.p.s spectra as well as solid phase $Na^+AsF_6^-$ spectra. We concentrate on the As(3*d*), F(1*s*), F(2*s*) and C(1*s*) peaks. The kinetic energies (relative to the F(1*s*) level) and the relative peak area ratios for these levels are tabulated in *Figure* 1 in graphical form for the AsF_5-doped materials.

For molecules in the gas phase[13], the relative areas under the peaks in the spectrum due to two levels i and j are:

$$R_{ij}(\text{gas}) = \frac{I_i}{I_j} = \frac{S_i N_i}{S_j N_j} \tag{1}$$

In equation (1) $S_i = T(E_i)\sigma_i$, where $T(E_i)$ is the transmission function of the instrument for electrons of kinetic energy E_i and σ_i is the photoionization cross section for level i, $N_i(x)$ is the number of atoms per unit volume of the species from which the ith electron is to be photoejected.

If a condensed phase sample is homogeneous (e.g., a condensed film of small molecules such as AsF_5) then:

$$R_{ij}(\text{cond.}) = \frac{S_i N_{i\lambda i}}{S_j N_{j\lambda j}} = R_{ij}\,(\text{gas})\,\frac{\lambda_i}{\lambda_j} \tag{2}$$

where $\lambda_i = \lambda(E_i)$ is the escape depth of the photoelectrons with kinetic energy E_i.

Consequently, comparing the peak intensity ratios for the $F(1s)$ and $F(2s)$ levels of the gas and condensed phases of AsF_5 and AsF_3 gives the ratio of the escape depths:

$$\frac{\lambda(1210\text{ eV})}{\lambda(560\text{ eV})} \approx 1.6 \tag{3}$$

For As(3*d*) and F(2*s*), however, the KE difference is only ~ 16 eV near 1200 eV, therefore their escape depths are nearly equal. Thus, the As(3*d*)/F(2*s*) peak area ratio is a measure of the chemical composition independent of an escape-depth effect. The data near the top of Column E of

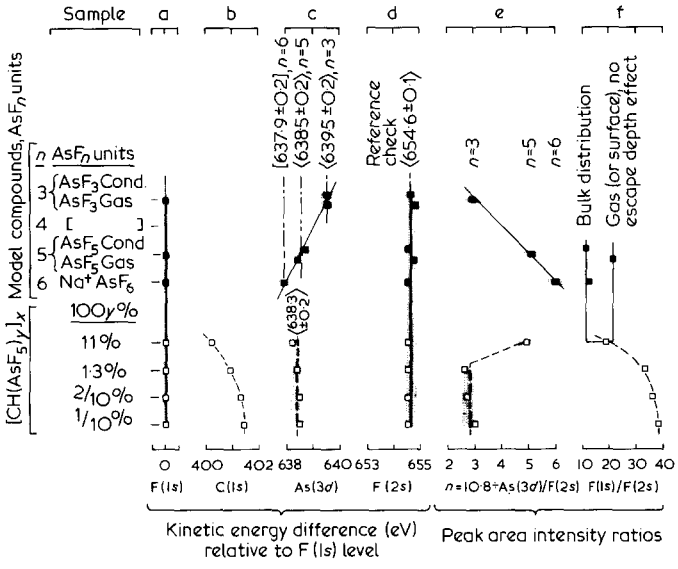

Figure 1 The core-level energy differences and relative peak area ratios for $[CH(AsF_5)_y]_x$ and various model molecules. For model compounds with AsF_n units, the value of n is shown in the sample column. Estimates of errors and/or reproducibility ranges are shown as cross hatched regions. The lettered columns establish: (A) fixed reference, (B) charge transfer, (C) As (3*d*) chemical shifts, (D) reference consistency check, (E) F:As intensity ratios, and (F) depth distribution effects. Some average values are given in brackets. Most data were obtained on from two to four samples[12].

Figure 1, shows that the As(3*d*)/F(2*s*) ratio is 10.8 ± 0.1 per F-atom, as determined from the model molecules with AsF_n units for $n=3$, 5 and 6. The data of Column F illustrates the escape depth effect on model compound solid films. We infer from these data that in $[(CH)(AsF_5)_{0.11}]_x$ the F:As ratio is 4.9 ± 0.1, in agreement with bulk chemical analysis.

The kinetic energy differences of the model compound core-levels are tabulated near the top of Columns (A)–(D) in *Figure* 1. Column C indicates the chemical shift observed for the As(3*d*) level when the number of F-atoms per As-atom varies in the range $3 \leqslant n \leqslant 6$, which is 0.53 ± 0.05 eV/F-atom. This shift is quite small, relative to carbon atoms, for which the value is about 2.5 eV/C-atom[13].

The doped polyacetylene samples exhibit an As(3*d*) line-width of ~ 2 eV, while the nearby F(2*s*) level, convenient for reference, has a width of ~ 3 eV. Therefore, the As(3*d*) chemical shift is observeable (Column C of *Figure* 1), but of sufficiently small magnitude relative to the line width as to render difficult the distinguishing of AsF_5 from, for example, AsF_6^- in doped-polyacetylene.

Additional information is obtained from the C(1*s*) core-level spectra. Relative to undoped $(CH)_x$, the C(1*s*) peaks move to higher binding energies by 0.6 ± 0.2 eV as shown in *Figure* 2, and indicated in Column B of *Figure* 1. The direction of the shift corresponds to charge transfer from the $(CH)_x$ to the arsenic–fluoride dopant. From Siegbahn's experimental tabulations[13], there is a 5.6 eV/electron chemical shift associated with the C(1*s*) level. Thus, 0.6 eV corresponds to 0.11 ± 0.01 electrons per C-atom, equivalent to about one electron per AsF_5 moiety.

(2) Valence level spectra: The interpretation of the valence electron photoemission and chemical shift data leads to the conclusion that the chemisorbed species are not 'simple' molecular entities like AsF_5 or AsF_5^- but rather are more complex species, e.g., $(As_2F_{10})^{2-}$, which exhibit a net As:F ratio near 1:5.

In *Figure* 3 we show the X-ray excited photoelectron spectra of pure $(CH)_x$, AsF_5-doped $(CH)_x$, gas-phase AsF_5 and condensed AsF_3. The energy scale of *Figure* 3 is that of gas phase AsF_5. The doped and pure $(CH)_x$ spectra are shifted by 4.1 eV, while the condensed phase AsF_3 spectra are shifted by 3eV, which is the observed shift of condensed AsF_5 relative to the gas phase. The differences between the spectra for AsF_3 and $[CH(AsF_5)_{0.11}]_x$ together with the similarities of those for AsF_5 and $[CH(AsF_5)_{0.11}]_x$ suggest that AsF_3 may not occur in appreciable concentration on the surface of the $(CH)_x$ fibrils.

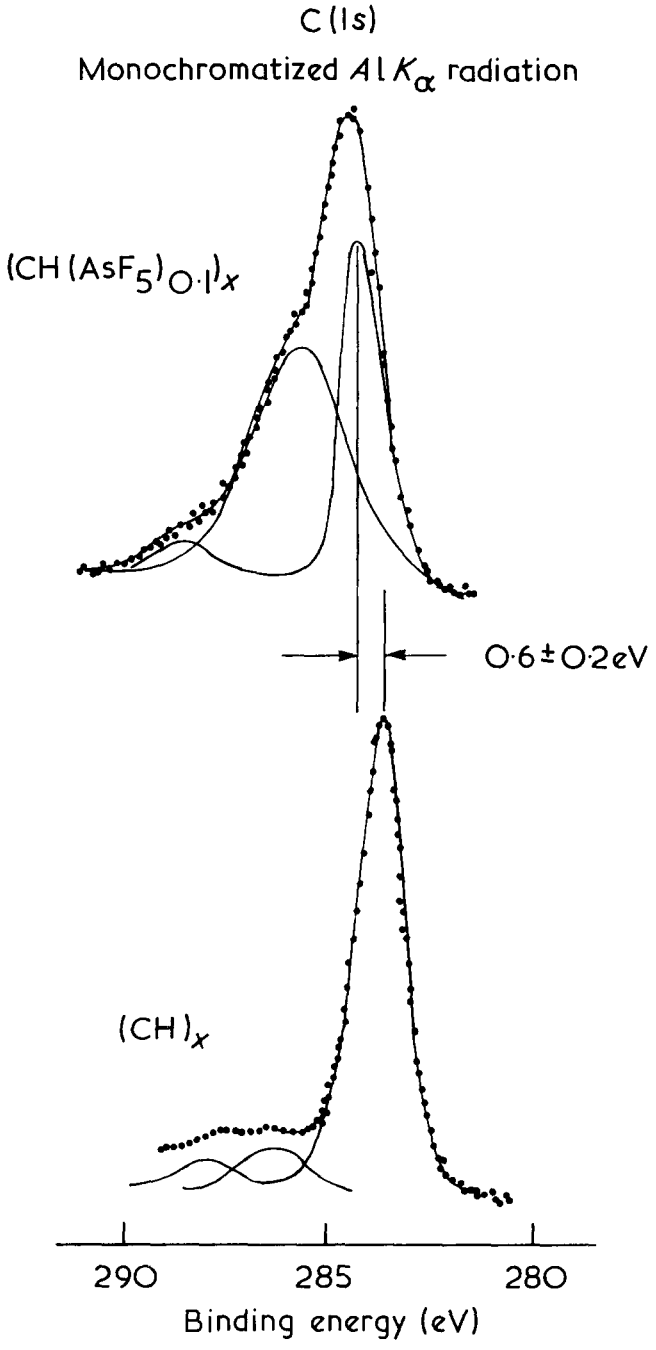

Figure 2 The C(1*s*) levels for pure (lower panel) and AsF_5-doped $(CH)_x$. The $\pi^* \leftarrow \pi$ transition typical of long chain polyenes appears as a weak shake-up peak about 2 1/2 eV to lower kinetic energy from the main C(1*s*) peak. The 'deconvolution' of the C(1*s*) spectrum for the doped polymer is for the purpose of locating the parent peak. The deconvolution of the satellite tail should not be taken literally[12].

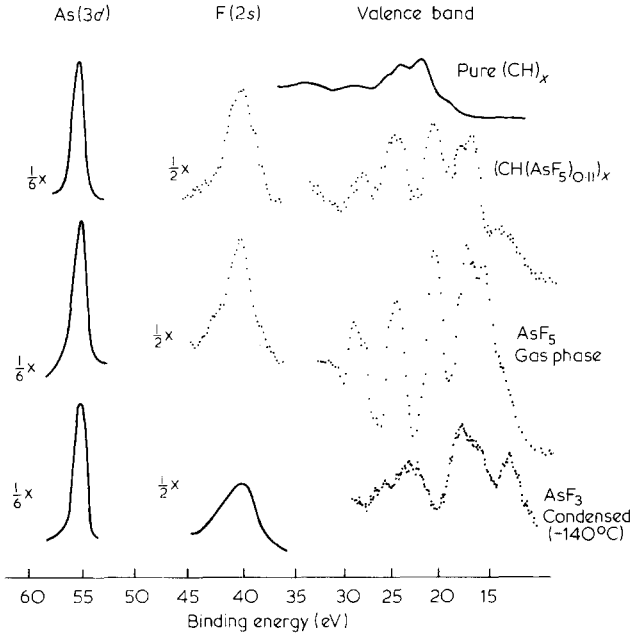

Figure 3 The highest kinetic energy portion of the X.p.s. shown for pure $(CH)_x$ (upper panel), AsF_5-doped $(CH)_x$, (second panel) AsF_5 molecules in the gas phase (third panel) and AsF_3 condensed on a gold substrate (bottom panel). The valence levels occur within the first 30 eV. The As(3*d*) and F(2*s*) core-level peaks are also shown. The binding energy scale is for AsF_5 in the gas phase. The other spectra were shifted to align the F(2*s*) and As(3*d*) peaks with those of the AsF_5 data. The magnitudes of the shifts are indicated in the figure[12].

The 40.8 eV photon energy u.p.s. spectra are shown in *Figure* 4. Note the 3.1 eV intermolecular relaxation energy shift obtained by comparing the AsF_5 gas phase and solid phase data. Between the AsF_5 condensed phase spectra and that of $[CH(AsF_5)_{0.11}]_x$, however, we find only a 1 eV shift.

The interpretation resulting from *Figures* 2–4 is, that following chemisorption of AsF_5, about one electron per As-atom is transferred from the highest occupied π-orbitals[14] of the $(CH)_x$ macromolecules to an as yet unspecified 'AsF_5' species. This interpretation is supported by comparison of the valence electron photemission from $[CH(AsF_5)_{0.11}]_x$ with that of AsF_5 and $(CH)_x$ as shown in *Figure* 3 and emphasized by *Figure* 4. The onset of photoemission, referenced to the cutoff of the secondary electron spectrum, occurs at 1.2 ± 0.15 eV higher binding energy (i.e. the work function increases) in $[CH(AsF_5)_{0.11}]_x$ as expected if electronic charge is withdrawn from low binding energy $(CH)_x$ molecular states. For $y = 0.11$, the semiconductor-to-metal transition in $[CH(AsF_5)_y]_x$ already has occurred, so the holes on the $(CH)_x$ backbone are not bound to the negatively charged 'AsF_5' species.

The most subtle aspect of the interpretation of our photoemission results is the identification of the electronic and chemical character of the final chemisorbed 'AsF_5' moiety. An important aspect of the valence electron spectra shown in *Figures* 3 and 4 is the general similarity of the valence electron photoemission spectra of AsF_5 and $[CH(AsF_5)_{0.11}]_x$ except for the appearance of a new (single hole-state) level at lower binding energy in $[CH(AsF_5)_{0.11}]_x$ relative to both $(CH)_x$ and molecular (gas phase or condensed) AsF_5. This level is marked by the arrow above the $[CH(AsF_5)_{0.11}]_x$ spectra in *Figure* 4. Inspection of *Figure* 3 reveals that there is almost no intensity in this energy region of the $(CH)_x$ X-ray valence electron spectrum (a consequence of the π-electron character of these states in $(CH)_x$[14]). Further evidence for this additional energy level is provided by the comparison, shown in *Figure* 5, of the highest kinetic energy portions of the fluorine KLL Auger spectra of $[CH(AsF_5)_{0.11}]_x$ with the corresponding spectra for molecular AsF_5. The basic features in the structure of the two Auger spectra are nearly identical except for the small (double holestate) peak in the $[CH(AsF_5)_{0.11}]_x$ spectrum which appears about 4.4 eV higher in kinetic energy than the highest peak in the AsF_5 spectrum. These data show that there is an additional occupied energy level in $[CH(AsF_5)_{0.11}]_x$ which has lower binding energy than the highest occupied orbital in the AsF_5 molecule, and has a finite amplitude to the F-atom. The simplest interpretation of these facts coupled with the observation of charge transfer from $(CH)_x$ is that the dopant is present as the radical anion, AsF_5^-, which exhibits an extra (half) filled electronic

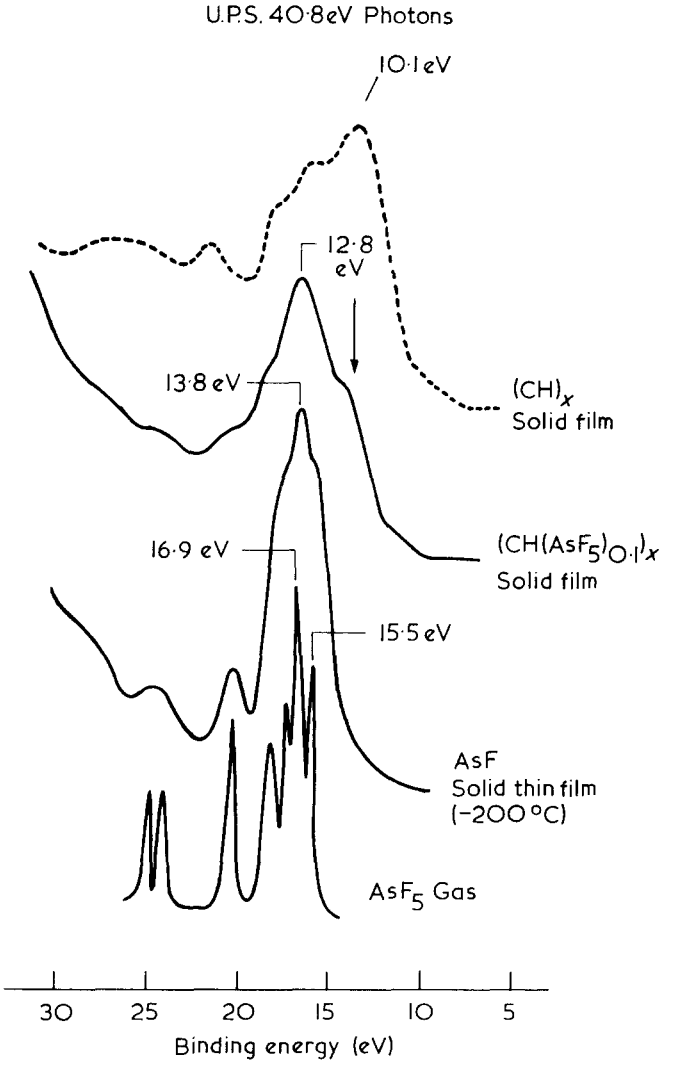

Figure 4 The 40.8 eV photon u.p.s. spectra for pure and AsF_5-doped $(CH)_x$, and for gaseous and condensed AsF_5. The various spectra have been shifted as indicated to align the major peaks in the spectra. The binding energy scale is for the AsF_5 gas phase spectrum[12].

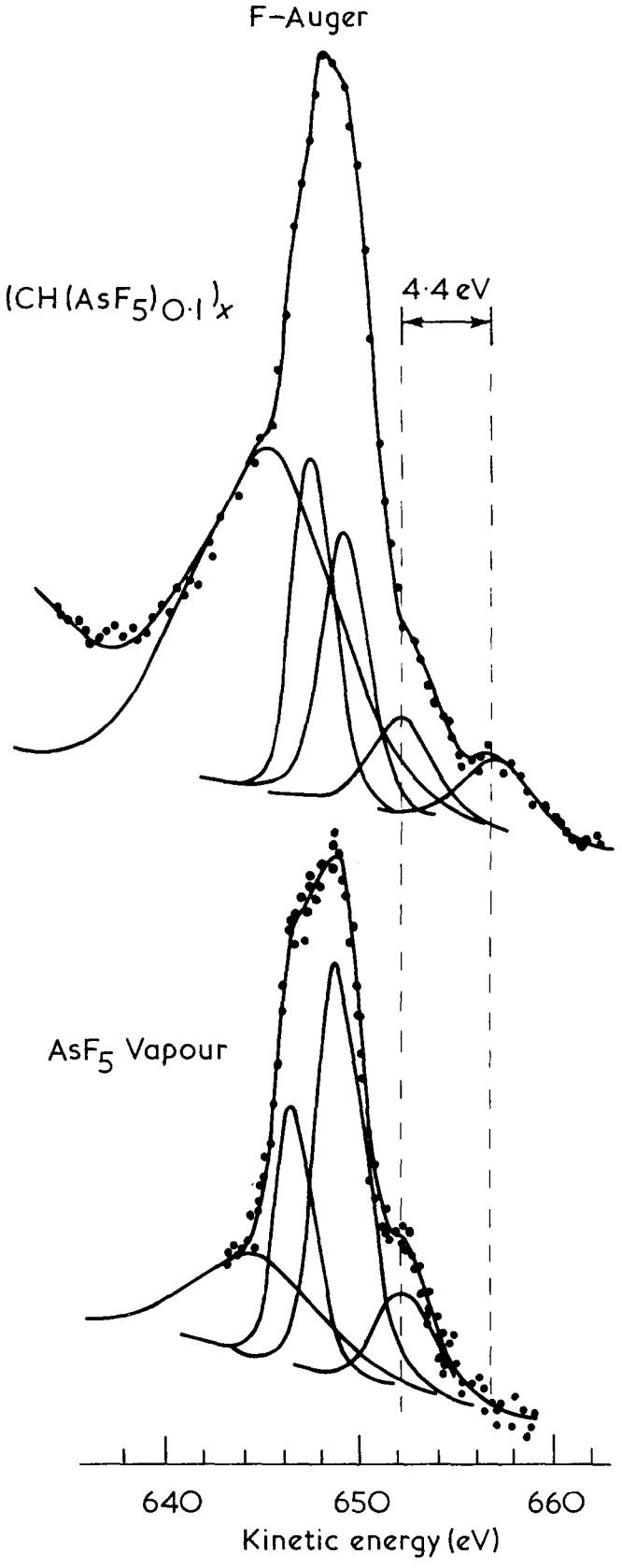

Figure 5 The fluorine KLL Auger electron spectra for AsF_5 molecules and the AsF_5-doped polymer. Note the appearance of the extra peak in the polymer data (arrow)[12].

orbital at an energy of ~2 eV above that of the orbital in AsF_5^- corresponding to the highest occupied orbital of neutral AsF_5.

This simple interpretation is, however, inconsistent with two other results. Firstly, static magnetic susceptibility measurements on $[CH(AsF_5)_y]_x$ have been carried out at several concentrations (y) both below and above the semiconductor-to-metal transition[15]. The principal result in the context of the present paper is that the observed susceptibility in the doped samples is temperature independent, whereas AsF_5^- would have an unpaired electron implying Curie law behaviour. Secondly CNDO/S3 calculations of the electronic structure of AsF_5, AsF_5^-, AsF_4^-, AsF_6^-, $(As_2F_{10})^{2-}$ and AsF_4H reveal that the highest occupied orbital of AsF_5^- lies in excess of 10 dV above the second-highest occupied orbital of the neutral molecule[16]. Consequently, even if molecular-ion-state relaxation effects are considered explicitly, the observed 2 eV splitting between the two uppermost ionization potentials is much too small for the case of AsF_5^-. It is noteworthy that the predicted[16] splitting of these ionizations is only 6.9 eV for $(As_2F_{10})^{2-}$, 1.4 eV for AsF_4 and zero for AsF_6^-. In addition, all of these species are diamagnetic. Therefore, on the basis of CNDO/S3 calculations, they can all be considered to be possible species which are consistent with both the photoemission and magnetic susceptibility data. One can also envisage more extended configurations of $(AsF)_{2n}^{2n-}$ in which the diamagnetism is caused by a Jahn–Teller instability in the chemisorbed AsF_5 near-surface layer[17]. Within this context, the positive charge (holes) may be either delocalized throughout the bulk of the $(CH)_x$ fibrils, or localized near a surface as in a depletion-layer-like surface state. The latter case would imply a high conductivity in the relatively small fractional volume of the surface region: a type of behaviour which may occur in the higher stages of intercalated graphite[18,19].

There has been another study of the As:F ratio in AsF_5-doped $(CH)_x$, carried out using hard X-ray absorption spectroscopy[20]. The major conclusion of this work is that the dopant becomes AsF_3 and AsF_6^- in the $(CH)_x$ with the majority of the AsF_3 being pumped off in the sample preparation process. Since the X-ray absorption measurement is bulk sensitive and the X.p.s. measurement is surface sensitive, it is possible that an inhomogeneous dopant identity throughout the fibril diameter could exist.

$(CHI_y)_x$ *for* y = 0.05, 0.12, 0.24 *and* 0.28

(1) Core level spectra: As described in detail elsewhere[21], the $I(3p_{3/2})$ and $I(3d_{3/2})$ of I_2 gas, I_2 condensed molecular solid film, and a sample of $(CHI_{0.05})_x$ are shown in *Figure* 6. The kinetic energy at which the 3*p* and 3*d* peaks are measured (with $MgK\alpha_{1,2}$ radiation) are different by about a factor of two. These two iodine core levels have the highest cross sections with reasonably narrow widths and were thus chosen for escape-depth analysis.

The I(3*d*):I(3*p*) intensity ratio is found to be about 3.0 $\pm$0.1 for I_2 molecules in the gas phase, and about 4.8 $\pm$ 0.1 for I_2 molecules in the condensed (solid) phase. These numbers were derived from spectra obtained with a $MgK\alpha_{1,2}$ X-ray source, and an angle of 90° between the photon propogation direction and the electron collection direction for both the gas and solid phase measurements. For all $(CHI_y)_x$ samples initially inserted into the spectrometer and cooled, the I(3*d*):I(3*p*) intensity ratio was found to be about 4.0 $\pm$ 0.2. After warming the samples to room temperature and pumping in the vacuum chamber overnight, the I(3*d*):(3*p*) ratio became ~3.5 $\pm$ 0.2. Both of these ratios are independent of the magnitude of the initial iodine concentration. From the gas phase and condensed

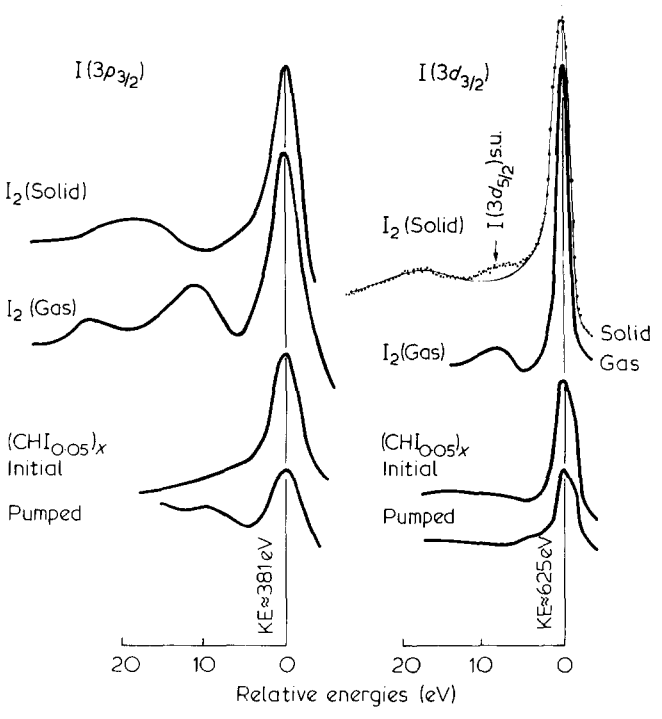

Figure 6 The I(3*p*) and I(3*d*) X.p.s. core level spectra for $(CHI_{0.05})_x$, I_2 gas, and condensed I_2. The approximate kinetic energies of the parent peaks are indicated for MgK $\alpha_{1,2}$ radiation. The dashed line on one $I(3d_{3/2})$ curve shows the residual after the shake-up ('s.u.') peak from the $I(3d_{5/2})$ peak is subtracted[21].

(solid) phase studies of I_2, we expect that a strictly surface layer of iodine on the $(CH)_x$ fibrils would yield an I(3*d*):I(3*p*) intensity ratio near 3.0, while an homogeneous distribution would yield a value near 4.8. The data initially indicate an approximately uniform distribution in the near-surface region, with some iodine preferentially removed from the surface region by the vacuum system when the samples are warmed to room temperature.

A second feature of *Figure* 6 is the shake-up satellite structure on the $3p_{3/2}$ and $3d_{3/2}$ peaks of iodine. The details of the shake-up on the iodine core levels are considered elsewhere[21]. The $3p_{3/2}$ peak exhibits a different satellite structure (to lower kinetic energies than the main peak) for I_2 molecules isolated in the gas phase as compared with those condensed in the (I_2) solid phase. The $I(3p_{3/2})$ peak for $(CHI_{0.05})_x$ tends to show a shake-up satellite similar to that for isolated I_2 molecules after some of the iodine is pumped away in the vacuum system (*Figure* 6, lower left-hand quadrant), although the $I(3d_{3/2})$ spectra do not follow the same trend. Therefore these spectra indicate the presence of species in addition to neutral I_2.

In *Figure* 7 the C(1*s*) spectra for pure $(CH)_x$ and for $(CHI_{0.28})_x$ along with the $I(3d_{5/2})$ spectrum for $(CHI_{0.28})_x$ after pumping are presented. These data were obtained at high resolution using monochromatic AlK $\alpha_{1,2}$ radiation. Consider first the $I(3d_{5/2})$ data. Note the deconvolution into two peaks. at ~619 eV and 620.5 eV (±0.2 eV) each with a shake-up peak to higher binding energy. The shake-up energies are slightly larger than the lowest energy $\pi^* \leftarrow \pi$ shake up transition observed on the C(1*s*) line for pure $(CH)_x$. Before removal of some iodine, the 620.5 eV peak was about twice the height of the 619 eV peak. Thus, the iodine removed from the sample corresponds predominantly to the 620.5 eV peak. Hsu, Signorelli. Pez and Baughman (HSPB) have observed the same peak splitting and subsequent decrease in the 620.5 (620.6 in their case) peak as discussed above[22]. They did not report, however, the two shake-up satellites shown here. HSPB determined that the 620.5 eV peak corresponds to I_2 and the 619.5 eV peak corresponds to I_3^-, by studying model iodine compounds, such as CsI_3. In conjunction with their Raman results and the lack of a large C(1*s*) chemical shift, HSPB conclude that iodine is present in $(CHI_{0.22})_x$ as I_5^-. Our data also indicate that an excess of I_2 is initially present, but vacuum removal of iodine results in almost equal peak heights and thus possibly only $I_2 + I_3^- = I_5^-$ as the major residual.

By working with a somewhat higher doping concentration than HSPB, we were able to observe a small shift in the C(1*s*) peak energy in iodine doped $(CH)_x$. A C(1*s*) chemical shift of 0.2 ± 0.2 eV (i.e. on the order of the experimental sample-to-sample reproducibility) is indicated in *Figure* 7. The shifts for smaller *y*-values were too small to be observed accurately. The magnitude of the C(1*s*) shift in $(CHI_{0.28})_x$ is in contrast to the shift to higher binding energies by ~0.6 eV for 10% doping of $(CH)_x$ with AsF_5 molecules[12]. This result for iodine, however, is consistent with the fact that AsF_5 is much more electronegative than I_2, as discussed below.

Siegbahn *et al.*[13] have shown that the C(1*s*) line exhibits a chemical shift slope of ~5.6 (±0.2) eV/electron. Our energy referencing scheme has been discussed previously[12]. The AsF_5-doped $(CH)_x$ results correspond to ~0.1 electrons per C-atom withdrawn from the polymer host. For iodine-doping, using Siegbahn's C(1*s*) slope and our reproducibility error bars, the charge transferred from

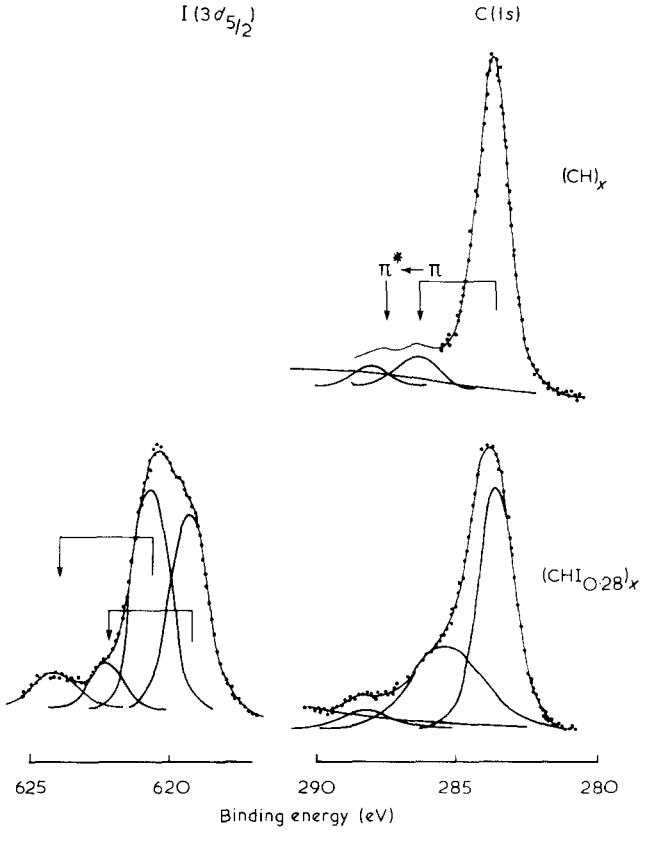

Figure 7 The C(1*s*) and $I(3d_{5/2})$ X.p.s. spectra for $(CHI_y)_x$ obtained at high resolution with monochromatized AlK $\alpha_{1,2}$ radiation. Energy calibration was achieved as discussed in reference 12. Details are discussed in the text[21].

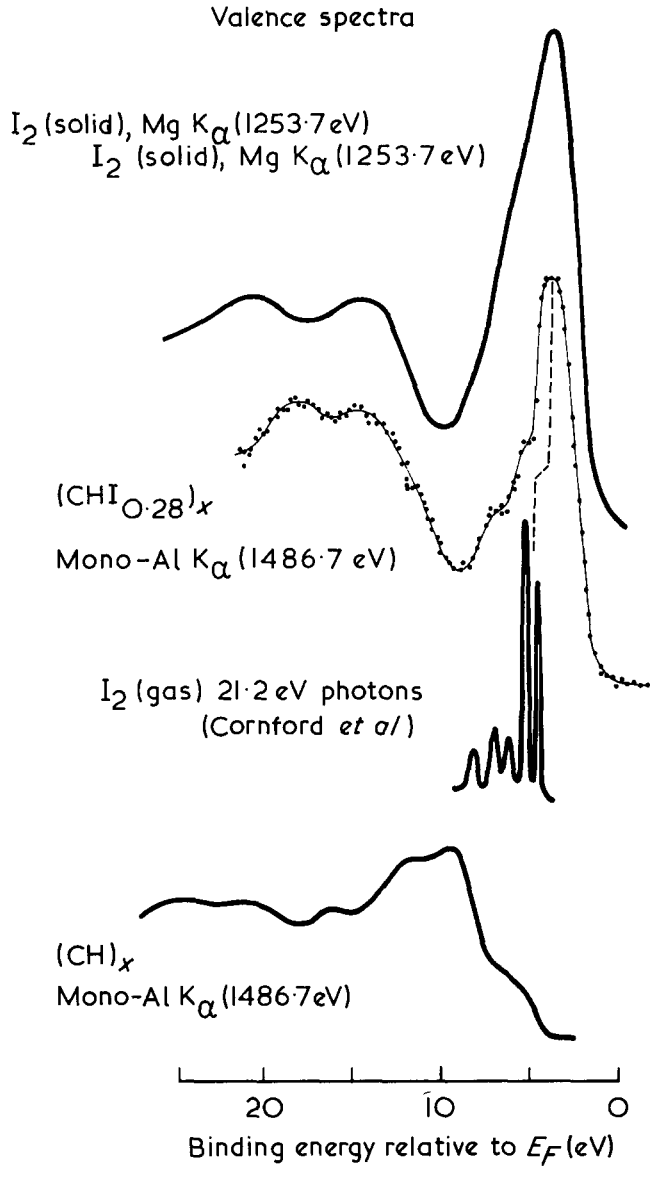

Figure 8 The X.p.s. valence spectra for pumped $(CHI_{0.28})_x$, condensed I_2, and I_2 in the gas phase[21,24].

the polymer host is no more than 0.03 electrons per C-atom. HSPB estimated an upper limit of 0.035 electrons per C-atom, a result with which we agree. Finally, the broadening of the C(1*s*) line for $(CHI_{0.28})_x$ is similar to that observed for AsF_5-doped $(CH)_x$, and is due to electronic excitations in the conducting polymer[12].

Both the I(3*d*) and the C(1*s*) spectra can be used, independently, to estimate the degree of charge transfer in the iodine–$(CH)_x$ complex. The direction of the shift in the C(1*s*) peak tells us that charge is transferred from the polymer host to the dopant species. For the degree of charge transfer, consider $(CHI_{0.28})_x$, for which the C(1*s*) chemical shift can be observed. After pumping, the composition is approximately $(CHI_{0.17})_x$. Rewriting the formula in terms of I_5^-, it becomes $(CH(I_5)_{0.03})_x$, allowing for a little residual I_2. The charge transfer as estimated from the shift of the C(1*s*) binding energy is $q \approx 0.03$ electrons per C-atom, in good agreement with $(CH(I_5)_{0.03})_x$. It appears, therefore, that each I_5^- has accepted one electron from ~33 C-atoms. It also seems that the $\pi^* \leftarrow \pi$ shake-up satellite of the C(1*s*) peak of pure $(CH)_x$ appears on the I(3*d*) peaks in iodine doped $(CH)_x$, while the C(1*s*) peak of iodine-doped $(CH)_x$ is broadened due to elementary excitations of the conducting polymer, as in the case of AsF_5-doped[12,23] $(CH)_x$.

(2) Valence level spectra: In *Figure* 8 the X.p.s. valence band spectra of pure $(CH)_x$, pumped $(CHI_{0.28})_x$ and a condensed film of I_2 are shown. A u.p.s. curve for I_2 vapour is also presented for comparison[24]. Pure *trans*$(CH)_x$ shows no significant X.p.s. signal intensity at the Fermi energy[12]. The C(2*p*)-derived MO's in this region have very low cross-section at X-ray photon energies. The iodine-doped sample shows a large increase intensity near E_F, but shows no finite signal at E_F. The X.p.s. valence spectrum of pumped $(CHI_{0.28})_x$ is very similar to that of condensed I_2, the main difference being the two maxima in the region of 15–20 eV. These maxima correspond to electrons photoemitted from the I(5*s*)-derived levels[21] of I_2, and have a somewhat different splitting in the doped-polymer than in pure I_2.

Assuming a work function of ~5 eV for solid I_2, the u.p.s. spectra are fixed with the first peak at 4.5 eV relative to the Fermi level (9.5 eV relative to the vacuum level)[24]. The energy difference between the sharp double-peak structure in the u.p.s. spectrum and the corresponding major maximum in the $(CHI_{0.28})_x$ spectrum is ~2 eV consistent with typical values of intermolecular relaxation energies[25]. Thus, there is no spectroscopic evidence for large charge transfer from the $(CH)_x$ in the valence band spectra. This is consistent with absence of a large C(1*s*) chemical shift.

In *Figure* 9 the u.p.s. spectra of pure[14] $(CH)_x$, pumped $(CHI_{0.28})_x$ and gas phase results of Cornford *et al.*[24] for I_2 are illustrated. All u.p.s. spectra are referenced to the vacuum level as determined by the cut-off of the secondary electron spectrum. The u.p.s. signal at the Fermi level does not indicate any large density-of-states at E_F; only a distinct onset of signal is observed. This result is consistent with the estimates of the density-of-states at E_F by static magnetic susceptibility measurements[15] and with the X.p.s. spectra on *trans*-$(CH)_x$ by HSPB[22]. The onset of our u.p.s. signal is found at the same value (4.5 ± 0.1 eV) in iodine-doped $(CH)_x$ as in pure $(CH)_x$[14] and is in contrast with the shifted onset observed[12] in 10% AsF_5-doped $(CH)_x$ (at 5.7 ± 0.1 eV). There is no spectroscopic evidence for Fermi level lowering in pumped $(CHI_{0.28})_x$ within the u.p.s. experimental uncertainty of 0.1 eV. It is also interesting that, in contrast to our X.p.s. valence band results, the u.p.s spectrum for pumped $(CHI_{0.28})_x$ does not have its major maximum shifted to lower kinetic energies compared with the u.p.s. spectrum of I_2 gas. The u.p.s. spectrum of pumped $(CHI_{0.28})_x$ looks more like that of pure $(CH)_x$. This result would argue against the surface localization of the iodine–dopant species after pumping, since the escape depths for electrons photogenerated with ultraviolet photons are consideralby less than those photogenerated by $AlK\alpha_{1,2}$ or $MgK\alpha_{1,2}$ X-radiation[26]. This u.p.s. result is consistent with the core-level results above.

Finally, the absence of a lowering of the Fermi level is consistent with doping of $(CH)_x$ through iodine induced soliton states[9–11]. Our measurements are not definitive, nor can they distinguish between soliton and one-electron models. The behaviour of the on-set to u.p.s. signal, however, is predicted within the framework of the soliton models. Since the generation of solitons via molecular doping results in energy states at the Fermi level, conductivity can occur without a lowering of E_F into the otherwise filled valence band.

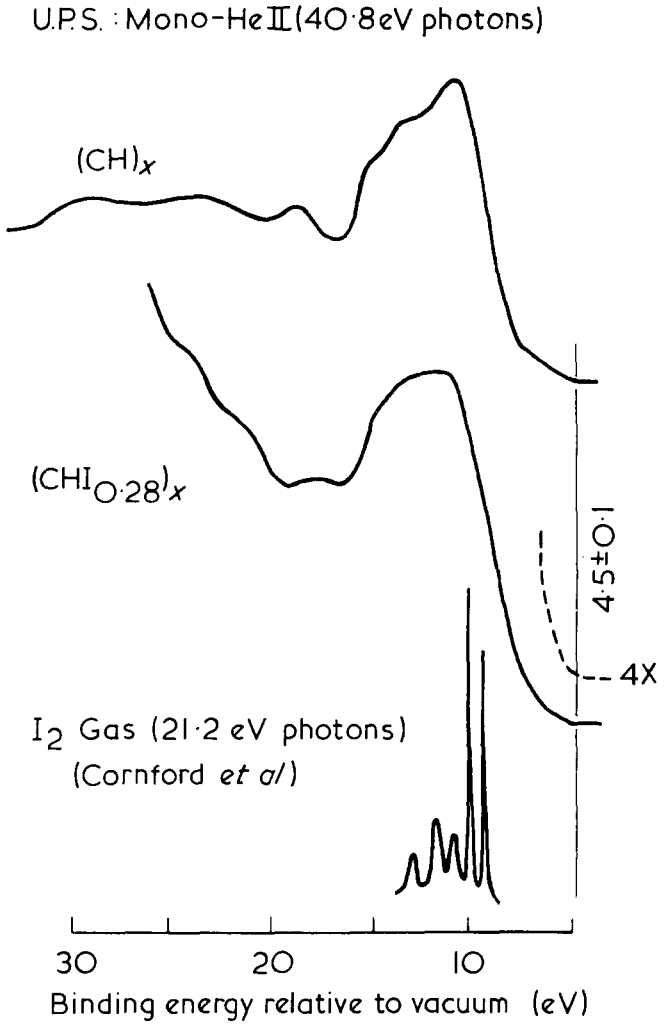

Figure 9 The u.p.s. spectra of $(CH)_x$ and pumped $(CHI_{0.28})_x$ obtained with monochromatized He II (40.8 eV photons) radiation. The gas phase He I (21.2 eV) spectrum for I_2 from reference 24 is shown for comparison[21].

SUMMARY

By measurement and interpretation of photoelectron and Auger electron spectra from $(CH)_x$, $[CH(AsF_5)_y]_x$, AsF_5, AsF_3, and $Na^+AsF_6^-$ we have established that in $[CH(AsF_5)_{0.11}]_x$ a fraction of the arsenic fluoride species lie near the surfaces of the $(CH)_x$ fibrils; the surface F:As atomic ratio is ~5; and that the arsenic fluoride does not occur as simple AsF_5^- anions even though about one electron per adsorbed AsF_5 moiety is transferred from the $(CH)_x$ fibrils to the arsenic fluoride species. From these results, we infer that the dopant species may exist in an ordered state and may induce an inhomogeneous charge distribution within the $(CH)_x$ fibrils due to the high conductivities observed in these materials[27]. At low dopant concentrations ($y < 0.1$) the F:As ratio is near 3, and the arsenic fluoride moieties are not obviously localized near the surface of the $(CH)_x$ fibrils. However, the spectra cannot establish that the dopant exists as AsF_3 moieties, due to the limitations discussed above.

Our results indicate that in $(CHI_y)_x$, the iodine initially present in the near-surface region (~30 to 50 Å) of the nominally 200 Å diameter $(CH)_x$ fibrils occurs as two parts I_2 to one part I_3^-. Vacuum pumping removes ~50% of the neutral I_2 leaving $I_2 + I_3^- = I_5^-$ as the probable complexed residual. The I_5^- complex would then account for one electron per five I-atoms, or a charge transfer of 0.03 electrons per C-atom. This result is consistent with the C(1*s*) chemical shift analysis, which indicates a nominal 0.03 electrons per C-atom charge transfer. LeFrant and coworkers have studied $(CHI_y)_x$ by Raman scattering and observed macroscopic inhomogeneous doping in their samples[28], while Mihaly and coworkers have obtained evidence of iodine dopant species distributed throughout the fibril bulk in the course of their n.m.r. studies[29] of $(CHI_y)_x$. It cannot be overemphasized that nominally X.p.s. probes only the outer 40 Å of the $(CH)_x$ fibrils and the pumping induced inhomogeneity is observed in this region.

Finally, the shape of the C(1*s*) X.p.s. peak in $(CH)_x$ changes by broadening on the lower kinetic energy side upon doping with iodine. This change is similar to that observed on the C(1*s*) line when $(CH)_x$ is doped with AsF_5 (but the peak energy shifts are different). The broadening is believed to be due to electronic excitations, generated in conjunction with the removal of an electron from the C(1*s*) level of $(CH)_x$ when doped to the highly conducting state[12].

Therefore we conclude that our photemission spectra are consistent with models in which the doping-induced increase in conductivity of molecularly doped $(CH)_x$ is caused by charge transfer from the $(CH)_x$ macromolecules to the dopant. The nature of the charged dopant species was established as I_5^- in (pumped) $(CHI_y)_x$ and as an unspecified moiety consistent with a 5:1 F:As ratio in the case of $[CH(AsF_5)_{0.11}]_x$. The identity of the mobile carriers in these materials (presumed to be either valence electron holes or domain-wall solitons in one-electron and collective-ground-state models, respectively)[9-11,27] cannot be established by photoelectron spectroscopy. Nevertheless, the continuous nature of their excitation spectra in the metallic regime is verified by the broadening of the C(1*s*) line. Our results are not definitive on whether or not a finite density of these states occurs at the Fermi energy for samples exhibiting metallic conductivity, although the very existence of metallic transport behaviour implies that such must be the case. Finally our spectra provide convincing evidence for inhomogeneous doping in $[CH(AsF_5)_{0.11}]_x$ but not in $(CHI_y)_x$, as well as a strong suggestion that the degree of inhomogeneity, and even the dopant species themselves, depend on the concentration of dopant. Comparison of the spectra with the predictions of simple models, of either the one-electron or collective-ground-state variety is made difficult by this inhomgeneous character of the doped material. Construction of more realistic theoretical models is required for quantitative data analysis.

ACKNOWLEDGMENTS

We thank Mr. Mark Druly for help in preparation of samples for the photoemission studies, Dr. J. Miller for supplying the $NaAsF_6$ samples, to Dr. Baughman for preprints, to Dr. A. Epstein and Dr. C. Beatty for valuable technical discussions, and to W. Greene for technical assistance.

REFERENCES

1 Shirakawa, H. and Ikeda, S. *Polymer J.* 1971, **2**, 231
2 Shirakawa, H., Ho, T. and Ikeda, S. *Polymer J.* 1973, **4**, 460
3 Ho, T., Shirakawa, H. and Ikeda, S. *J. Polym. Sci. Polym. Chem. Ed.* 1974, **12**, 11; 1975, **13**, 1943

4 Chiang, C. K., Fincher, C. R. Jr., Park, Y. W., Heeger, A. J., Shirakawa, H., Louis, E. J., Gau, S. C. and MacDiarmid, A. G. *Phys. Rev. Lett.* 1977, **39**, 1089

5 Chiang, C. K., Druy, M. A., Gau, S. C., Heeger, A. J., Louis, E. J., MacDiarmid, A. G., Park, Y. W. and Shirakawa, H. *J. Am. Chem. Soc.* 1978, **100**, 1013

6 Chiang, C. K., Gau, S. C., Fincher, C. R. Jr., Park, Y. W., MacDiarmid, A. G. and Heeger A. J. *Appl. Phys. Lett.* 1978, **33**, 18

7 Chiang, C. K., Park, Y. W., Heeger, A. J., Shirakawa, H., Louis, E. J. and MacDiarmid, A. G. *J. Chem. Phys.* 1978, **69**, 5098

8 Park, Y. W., Drury, M. A., Chang, C. G., MacDiarmid, A. G., Heeger, A. J., Shirakawa, H. and Ikeda, S. *J. Polym. Sci.: Polym. Lett. Ed.* 1975, **17**, 195

9 Rice, M. J. *Phys. Lett.* 1979, **71A**, 152

10 Su, W. P., Schreiffer, J. R. and Heeger, A. J. *Phys. Rev. Lett.* 1979, **42**, 1698

11 Duke, C. B. in 'Extended Linear Chain Conductors' (Ed. J. S. Miller) Plenum Press, New York 1980, in press

12 Salaneck, W. R., Thomas, H. R., Duke, C. B., Paton, A., Plummer, E. W., Heeger, A. J. and MacDiarmid, A. G. *J. Chem. Phys.* 1979, **71**, 2044

13 Siegbahn, K., Nordling, C., Johansson, G., Hedman, J., Heden, P. F., Hamrin, K., Gelius, V., Bergmark, T., Werme, L. O., Manne, R. and Baer, Y. 'ESCA Applied to Free Molecules' North Holland, Amsterdam 1969, p 114

14 Duke, C. B., Paton, A., Salaneck, W. R., Thomas, H. R., Plummer, E. W., Heeger, A. J. and MacDiarmid, A. G. *Chem. Phys. Lett.* 1978, **59**, 146

15 Goldberg, I. B., Crowe, H. P., Newman, P. R., Heeger, A. J. and MacDiarmid, A. G. *J. Chem. Phys.* 1979, **70**, 1132

16 Duke, C. B. and Paton, A. to be published

17 Duke, C. B., Lubinsky, A. R., Lee, B. W. and Mark, P. *J. Vacuum Soc. Tech.* 1976, **13**, 761

18 Spain, I. L. and Nagel, D. J. *Mater. Sci. Eng.* 1977, **31**, 183

19 Batallan, F., Bok, J., Rosenmann, I. and Melin, J. *Phys. Rev. Lett.* 1978, **41**, 330

20 Clarke, T. C., Geiss, R. H., Gill, W. D., Grant, P. M., Macklin, J. W., Morawitz, H., Rabolt, J. F., Street, G. D. and Sayers, D. *J. Synth Metals* 1979, **1**, 21

21 Salaneck, W. R., Thomas, H. R., Duke, C. B., Bigelow, R. W., Plummer, E. W., Heeger, A. J. and MacDiarmid, A. G. *J. Chem. Phys.* 1980, **72**, 3674

22 Hsu, S. L., Signorelli, A. J., Pez, G. P. and Baughman, R. H. *J. Chem. Phys.* 1978, **69**, 106

23 Salaneck, W. R., Thomas, H. R., Duke, C. B., Plummer, E. W., Heeger, A. J. and MacDiarmid, A. G. *J. Synth. Metals* 1979, **1**, 133

24 Cornford, A. B., Frost, D. C., McDowell, C. A., Ragle, J. L. and Stenhouse, I. A. *J. Chem. Phys.* 1971, **54**, 2651

25 Duke, C. B., Salaneck, W. R., Paton, A., Liang, K. S., Lipari, N. O. and Zallen, R. in 'Structure and Excitations of Amorphous Solids', (Eds G. Lucovsky and F. L. Galeener) American Institute of Physics, New York, 1976, pp. 23–30

26 Carter, W. J., Schweitzer, G. K. and Carlson, T. A. *J. Electron Spectros.* 1974, **5**, 827

27 Fincher, C. R. Jr., Ozaki, M., Heeger, A. J. and MacDiarmid, A. G. *Phys. Rev.* 1979, B **19**, 4140

28 Lefrant, S., Lichtman, L. S., Temkin, H., Fitchen, D. B., Miller, D. C., Whitewell, G. E. and Burlitch, J. M. *Solid State Commun.* 1979, **29**, 191

29 Mihaly, L., Pekker, S. and Janossy, A. to be published